Desalination and Water Treatment
www.deswater.com

doi: 10.5004/dwt.2020.25345

184 (2020) 178–188
April

Heavy metal adsorption efficiency magnetic porous composites Fe_3O_4–SiO_2–APTES

Leila Karimi Takanlou[a,b], Mahdi Farzadkia[a,b,*], Amir Hossein Mahvi[c,d], Ali Esrafili[a,b]

[a]*Research Center for Environmental Health Technology, Iran University of Medical Sciences, Tehran, Iran, Tel. +98-21-88779118; emails: farzadkia.m@iums.ac.ir (M. Farzadkia), lkarimi21@yahoo.com (L.K. Takanlou), a_esrafily@yahoo.com (A. Esrafili)*

[b]*Department of Environmental Health Engineering, School of Public Health, Iran University of Medical Sciences, Tehran, Iran*

[c]*School of Public Health, Tehran University of Medical Sciences, Tehran, Iran*

[d]*Center for Solid Waste Research, Institute for Environmental Research, Tehran University of Medical Sciences, Tehran, Iran, email: ahmahvi@yahoo.com (A.H. Mahvi)*

Received 27 March 2019; Accepted 13 December 2019

ABSTRACT

Heavy metals such as Cd^{2+} and Ni^{2+} in water have been a major issue for many years. This study presented heavy metal adsorption efficiency by Fe_3O_4–SiO_2 and Fe_3O_4–SiO_2–APTES. Fe_3O_4–SiO_2 synthesized by sol-gel method and was modified with APTES. Characteristics of adsorbents, including particle structure, composition and size were determined using analytical devices such as XRD, scanning electron microscopy, Fourier transform infrared spectra. In order to design experiments and analyse the results, the Software Design-Expert 7 and Taguchi method was used. Physical and chemical parameters such as pH, contact time, and adsorbent dosage under various conditions were studied. The result shows that in pH ≥ 5.5–6.5, initial Cd^{2+} and Ni^{2+} with 10 mg/L concentration, 20 mg adsorbent dosage, and 20 min contact time, resulted in 75.5% cadmium and 70.5% nickel removal by Fe_3O_4–SiO_2. Moreover, the maximum capacity of cadmium and nickel adsorption was achieved 18.88 and 17.63 mg/g of adsorbent, respectively. In optimal condition (pH ≥ 6.5–7, 10 mg/L initial cadmium and nickel concentrations, 20 mg adsorbent dosage, 10 min contact time), 95.5% of cadmium and 83.5% of nickel were removed from solutions, respectively. In addition, the maximum adsorption capacity of Fe_3O_4–SiO_2–APTES for cadmium and nickel adsorption was 22.63 and 20.88 mg/g, respectively. While, Fe_3O_4@SiO_2 shows the maximum adsorption capacity of 18.88 and 17.63 mg/g for cadmium and nickel, respectively. The adsorption isotherm follows both of the Langmuir and Freundlich models (R^2 > 0.97). Finally, Fe_3O_4–SiO_2–APTES have more ability than Fe_3O_4–SiO_2 to quickly and efficiently adsorb nickel and cadmium ions. In addition, modified magnetic silicon nanoparticle can be industrially used as reusable and environment friendly adsorbent.

Keywords: Adsorption; Cadmium; Nickel; $FeSO_4$@SiO_2; Ligand

1. Introduction

Heavy metals such as lead, mercury, copper, zinc and cadmium are the main group of inorganic contaminants in aquatic system, which are known as a carcinogen, so they are major concerns in recent years [1]. It is demonstrated that long-term water consumption that contains heavy metals leads to cancer and nervous system damages, etc. [2]. Therefore, removal of ion metal from contaminated water and wastewater is necessary due to health hazards and environmental protection [3–5]. That is reported that heavy metals are generally released into the environment as a result of manufacturing, pharmaceutical, industrial, agricultural chemicals, and anthropogenic activities [6]. Although, any

* Corresponding author.

metal species should be considered as contaminant but nickel and cadmium are the most important part in water and wastewater posing significant hazards to human, animal, and ecosystem health [7]. For example, itai-itai disease is caused by cadmium pollution. Rising demands for clean and safe water with extremely low levels of heavy metal ions make it greatly important to develop improved technologies for heavy metal ions removal. Heavy metals are the compounds that cannot be degraded biologically similar to organic pollutants, so removing them needs special treatment methods. Some of the main methods which have been used for removing heavy metal from water and wastewater are including oxidation, reduction, precipitation, membrane filtration, ion exchange, adsorption and electrocoagulation [8–13]. These methods have several disadvantageous features such as expensive equipment requirement, continuous replenishment of chemicals, time consuming and easy to produce secondary pollution. Considering the limitations of conventional methods for metal ions removal, the most promising alternative method appears to be the optimal adsorption process. However, among various suggested methods, adsorption is one of the preferred method for the removal of metal ions from water and wastewater because it is a simple operation, cost effective and environmental friendly method [13]. In the last few decades, various adsorbents have been developed [14–16]. However, nowadays application of nanotechnology as a nanoadsorbent has been considered [17]. Silicon nanoparticles due to unique properties such as least toxicity, biodegradable and environmental friendly have been largely used in the water and wastewater purification [18–21]. Some research have been reported that a modified large pore size mesoporous silica shell with a magnetic core (Fe_3O_4) can improve efficiency sensing removal of heavy metal in adsorption process [22]. Numerous researches carried out around this area of study. Anbia et al. [23] used modified magnetic mesoporous MCM-48 silica, for removal of Pb^{2+}, Cu^{2+}, Cr^{2+} and Cd^{2+} metal ions from aqueous solutions. Yuan et al. [24] applied magnetic core (Fe_3O_4) on the silica shell for improving effective adsorption and removal of heavy metal ions. Meanwhile, in some other document magnetic porous composites modified with amino groups have been used to remove heavy metals from wastewater [25]. Sahoo et al. [26] have used hexa-dentate ligand-modified magnetic nanocomposites to remove heavy metals. Although, there are researches on the application of adsorption in the environmental area by magnetic nanoparticles, there are some reports on the preparation of APTES functionalized mesoporous magnetite and application on the adsorptions of heavy metal ions onto mesoporous magnetic nanoparticles. In addition, previous studies on silica being supported by different material such as sulfuric acid, chloride, acetic acid were used but some of these methods suffer from disadvantage such as long reaction time, unsatisfactory yield and toxic organics. Thus, development of efficient, easy, high yielding and ecofriendly method would be highly desirable. Here, magnetic porous composites (Fe_3O_4–SiO_2) modified with APTES ligand was used as a nanoadsorbent to remove Ni^{2+} and Cd^{2+} ions from aqueous solutions. Also, the effect of a few factors including pH, initial metal ion concentration, adsorbent dosage and contact time on the adsorption process has been investigated and the regeneration test was also performed to investigate application efficiency.

2. Experiments

2.1. Reagents and instrument

All of the chemical reagents, including ferrous chloride tetrahydrate ($FeCl_2{\cdot}4H_2O$), ferric chloride hexahydrate ($FeCl_3{\cdot}6H_2O$), ammonia (NH_3), cadmium nitrate tetrahydrate ($Cd(NO_3)_2{\cdot}4H_2O$), nickel nitrate ($Ni(NO_3)_2$), ethanol (C_2H_5OH), hydrochloric acid (HCl), nitric acid (HNO_3), and sodium hydroxide (NaOH) were purchased from Merck (Darmstadt, Germany, >99% purity). Stock solutions (1,000 mg L^{-1}) were prepared by dissolving solid cadmium nitrate tetrahydrate and nickel nitrate in distilled water, then various concentrations (1–20 mg L^{-1}) were also prepared. Initial pH of each solution was adjusted by pHs-3C model acidity meter (Shanghai Precision & Scientific Instrument Co. Ltd., China). $Cd^{2+}$and Ni^{2+} concentrations were measured by atomic absorption spectrophotometer (PerkinElmer Analyst 200, Mundelein, Illinois 60060 USA). The structure and morphology of synthesized composed were investigated by scanning electron microscopy (SEM). The distribution of elements was determined via energy-dispersive spectroscopy. Fourier transform infrared spectra (FT–IR) were recorded in KBr pellets with a Nicolet 5700 spectrometer (Madison, WI USA).

2.2. Synthesis of Fe_3O_4 nanoparticles

Fe_3O_4 nanoparticles were prepared by adding 8.48 g of iron (III) chloride hexahydrate ($FeCl_3{\cdot}6H_2O$) in 5.25 g of iron (II) chloride heptahydrate ($FeCl_2{\cdot}7H_2O$) then dissolved in 400 mL distilled water, then, was stirred vigorously under an N_2 atmosphere at 80°C for 1 h. Finally, 26% ammonium hydroxide was added into the mixture and was stirred. Produced nanoparticles were washed with deionized water.

2.3. Synthesis of Fe_3O_4@SiO_2 nanoparticles

Co-precipitation method was used for preparing Fe_3O_4@SiO_2. First, 11.68 g $FeCl_3{\cdot}6H_2O$ and 4.30 g $FeCl_2{\cdot}4H_2O$ were dissolved in 400 mL deionized water and was sonicated to get a uniform dispersion at 85°C under N_2 atmosphere. Subsequently, ammonium hydroxide (20 mL) was added to the solution. Produced magnetic fluid was dispersed and was washed with deionized water (0.02 mol/L) and sodium chloride. Finally, 10% (v/v) of tetraethyl orthosilicate (TEOS) was added via the equivalently fractioned drop method. Then solution pH solution was adjusted to 4.6 and mixtures were stirred mechanically for 2 h at 90°C. Finally, Fe_3O_4@SiO_2 core–shell NPs were collected after centrifuging and washing, and then were dispersed in ethanol.

2.4. Synthesis of Fe_3O_4@SiO_2–APTES nanocomposites

For preparing Fe_3O_4@SiO_2–APTES, 10 g magnetic porous composites (Fe_3O_4@SiO_2) were mixed with 3 mL APTES at room temperature for 12 h. Finally, the resulting product was isolated by magnetic separation, washed with ethanol, and dried in vacuum under 80°C for 12 h.

2.5. Batch adsorption experiments

Experiments were carried out according to the Standard Methods for Examination of Water and Wastewater [27]. Batch adsorption studies were conducted to determine effect of each variable pH (3,5,7,9), contact time (10, 20, 30, 40 min), initial concentration of Cd^{2+} and Ni^{2+} (1, 5, 10, 50 mg/L) stirring speed (100, 200, 300, 400 rpm) and adsorbent dosage (0.05, 0.1, 0.5, 1 mg/L). The optimum adsorption conditions were obtained by varying each variable while others kept constant. Finally, adsorption isotherm (Langmuir and Freundlich isotherm models) was determined in the optimum condition, which was achieved.

2.6. Statistical analysis

Experiments were conducted based on the mean ± standard deviation (SD). Adsorption efficiency of heavy metal on the Fe_3O_4–SiO_2 modified with APTES legend was analysis by using SPSS 17.00 Windows version and the obtained data were analyzed using ANOVA test.

3. Result and discussion

3.1. Characterization of Fe_3O_4 and Fe_3O_4@SiO_2 NPs

Morphologies of synthesized Fe_3O_4 and Fe_3O_4@SiO_2 NPs were determined by scanning electron microscope and are illustrated in Figs. 1a and b, respectively.

The obtained result shows that although Fe_3O_4@SiO_2 has a same morphology similar to Fe_3O_4, slightly larger particle size and smoother surface is observable. To explain this difference, it may be related to uniform coating of silica onto the Fe_3O_4 nanoparticles. In addition, the obtained larger particle size is due to aggregation of small crystallites through synthesis [28]. Fig. 2 exhibits FT–IR spectra of synthesized nanoparticle Fe_3O_4 (a), Fe_3O_4@SiO_2 (b) and Fe_3O_4@SiO_2–APTES (c). As it can be clearly seen in the following image, Fe_3O_4 nanoparticle shows a strong peak on the 1,717 and 1,637 cm^{-1} which is related to vibration of C=C band and C=O band, respectively. While FT–IR spectra of Fe_3O_4@SiO_2 decorated two weak peaks on the 1,703 and 1,639 cm^{-1} that are attributed to C=O and C=C, respectively, and indicate that surface of nanoparticle has been successfully functioning. Also, absorption bands of OH (3,470 cm^{-1}), Fe–O–Fe (590 cm^{-1}) groups are observed. Moreover, the vibration band at 1,034 and 1,125 cm^{-1} attributed to the SiO–H and Si–O–Si groups, another vibration peak at the 3,470 and 1,632 cm^{-1} assigned to NH_2 bending mode of free NH_2 group, respectively [29]. The FTIR spectrum of the APTES–SiO_2–magnetite confirm two broad bands at 1,629 and 1,574 cm^{-1} which are related to C=O stretching vibration. The absorption bands of CH_2 (2,800 cm^{-1}), C–O (1,311 cm^{-1}) and C–N (1,055 cm^{-1}) groups are observed [30]. According to the obtained result from Fig. 3, Fe_3O_4 (a), Fe_3O_4@SiO_2 (b) were characterized by energy dispersive analysis of X-ray (EDX). The result of EDX spectrum prevalent that the Fe (92.11%) and O (7.89%) are the only elementary components of Fe_3O_4 nanoparticles. Furthermore, EDX spectrum of Fe_3O_4@SiO_2 shows that the elemental compositions are Fe (%27.95), O (36.73%), and Si (35.32%) of core-shell nanoparticles.

3.2. Effect of initial pH on adsorption

A surface charge of Fe_3O_4, Fe_3O_4@SiO_2 and Fe_3O_4@SiO_2–APTES was determined by pH pzc (Fig. 4). The effect of pH on Cd^{2+} and Ni^{2+} capacity of adsorption by varying the pH (3–9) at 40 min was investigated. It was observed that the adsorption efficiency was increased with increasing pH from 3 to 6, also it was decreased at pH > 6. Moreover, maximum absorption efficiency for Ni^{2+} and Cd^{2+} was 70.5% and 75.5%, respectively. Meanwhile, adsorption capacity was determined to be 17.63 and 18.88 mg/g for Ni^{2+} and Cd^{2+}, respectively. While, minimum adsorption capacity of Ni^{2+} (37.43 mg/g) and Cd^{2+} (11.15 mg/g) was observed at the pH = 3. It was observed that high adsorption efficiency was obtained at pH = 3–7 range; while, it was a remarkable decrease at pH > 6. In addition, it was negligible in neutral pH (Fig. 5b). Fig. 5b demonstrates the pH effect on the Fe_3O_4@SiO_2–APTES nanoparticle

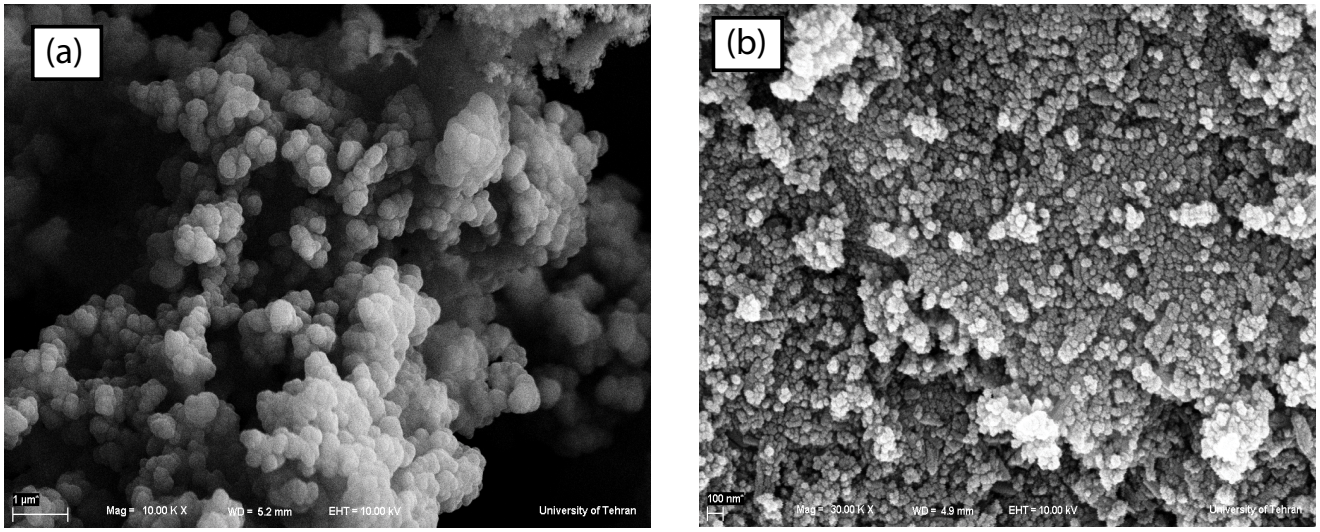

Fig. 1. SEM image of Fe_3O_4 (a) and Fe_3O_4@SiO_2 NPs (b).

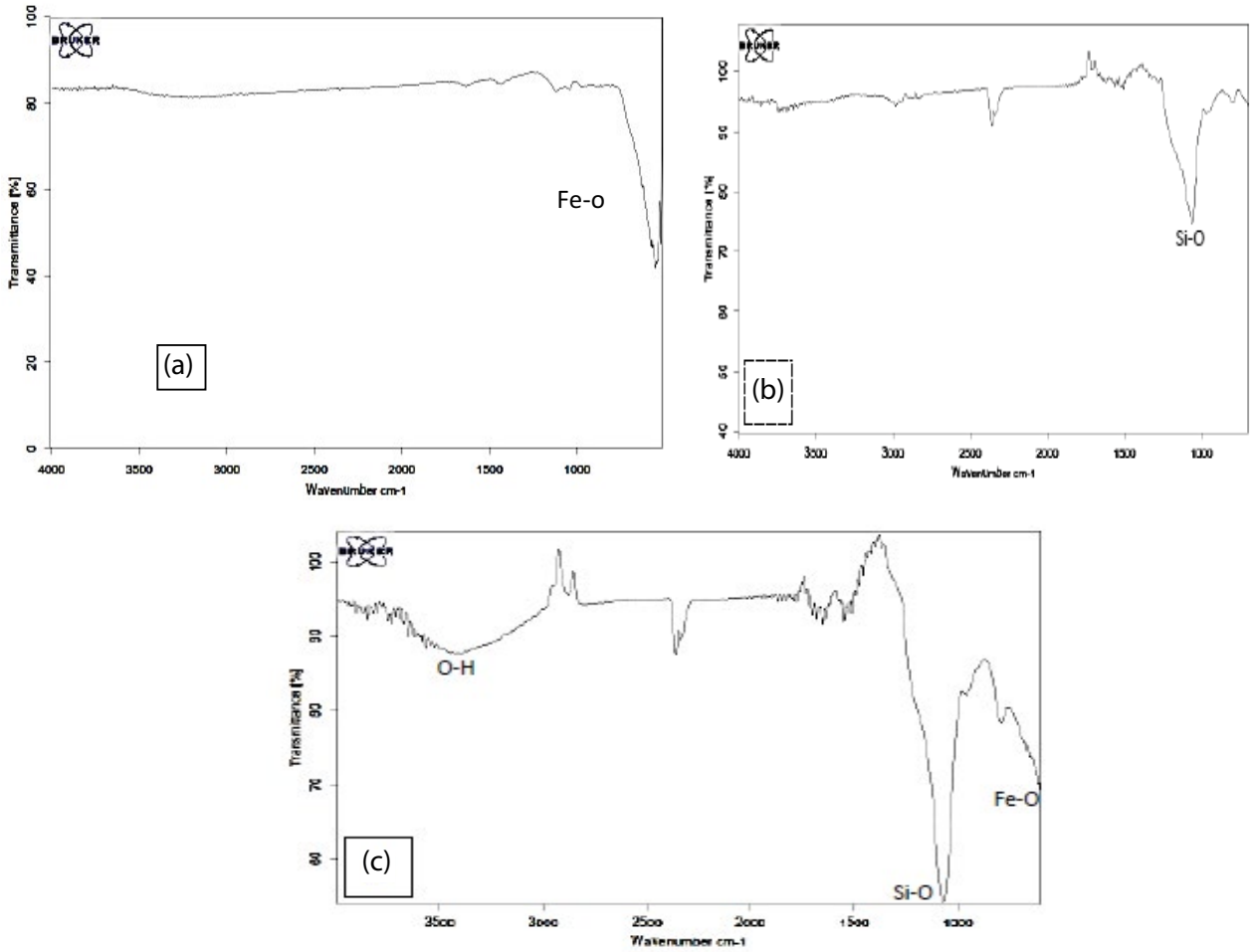

Fig. 2. FT–IR spectra of nanoparticle Fe_3O_4 (a), Fe_3O_4@SiO_2 (b) and Fe_3O_4@SiO_2–APTES (c).

adsorption efficiency. The adsorption efficiency increased when the solution pH value increased above 6, and the largest removal is over 90.5% and 83.5% for Cd^{2+} and Ni^{2+}, respectively, at pH = 7. Moreover, the adsorption can be affected by the formation of the respective hydroxide precipitates at pH > 7.5. So, precipitated metal hydroxide gets out from the solution [31]. Some research have reported that adsorption process at the pH 6–6.5 following electrostatic adsorption can increase removal of heavy metal (85%) [32,33]. While, other researchers reported that highest removal efficiency of metal ion has been obtained at pH ≥ 5.5. In a further related study, Cheng et al. [34] also reported on the highest efficiency of Pb^{+2} removal occuring at pH < 6. Banerjee and Chen [35] have used Fe_3O_4-gum-arabic nanocomposite for removal of Cu^{2+} and also have reported that at pH 2–6 adsorption increases with increase in pH. Moreover, effect of pH and adsorbent dosage of Fe_3O_4@SiO_2 (a) and Fe_3O_4@SiO_2–APTES (b) on the removal efficiency of the target ions is shown in Fig. 6.

3.3. Effect of contact time on the adsorption

The experiment about the effect of contact time on the adsorption was carried out on overall 40 min and it was determined that the adsorption efficiency of Fe_3O_4@SiO_2 was increased with increasing contact time. In addition, obtained data show that adsorption has a sharp increasing trend within the first 20 min; while, it decreased from 20 to 30 min due to desorption then, it has constant adsorption until reaching equilibrium in 40 min. Therefore, equilibrium time was reported to be 30 min. The target ions can easily diffuse into the small pore size of Fe_3O_4@SiO_2 and Fe_3O_4@Si@APTES NPs resulting in the maximum adsorption attained within 20 min (Fig. 7). In addition, it should be mentioned that a large number of vacant active sites were still available for the adsorption during the initial time [36]. However, affect the nature of the adsorbent and its available adsorption sites on the equilibrium time undeniable [37]. Some documents have reported that decreasing heavy metal removal efficiency by increasing contact time is due to decreasing strength of sorption and/or the breaking of the sorbate-surface bond [38]. Meanwhile others reported that other factors such as increase in agitation time could increase the cadmium uptake [39].

3.4. Effect of adsorbent dosage

Effect of dosage is an important factor in the adsorption process and optimum adsorbent dosage can enhance

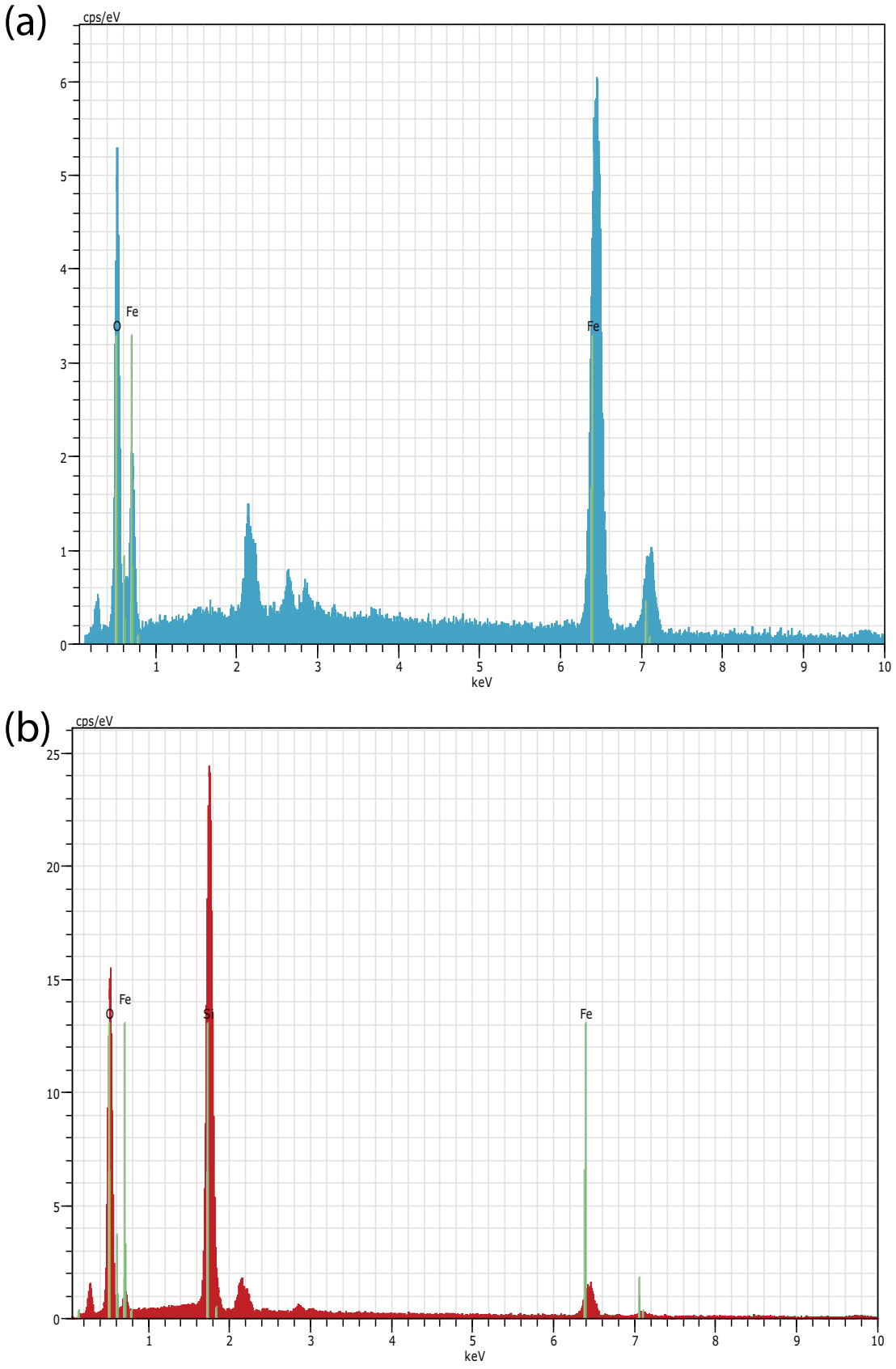

Fig. 1. EDX spectrum of Fe_3O_4 (a), Fe_3O_4@SiO_2 (b).

interactions between metal ions and surface adsorption site of adsorbent [40]. As shown in Fig. 8, concentrations of Cd^{2+} and Ni^{2+} ion in the solution were gradually decreased with increasing adsorbent dosage from 5.00 to 100 g L^{-1}.

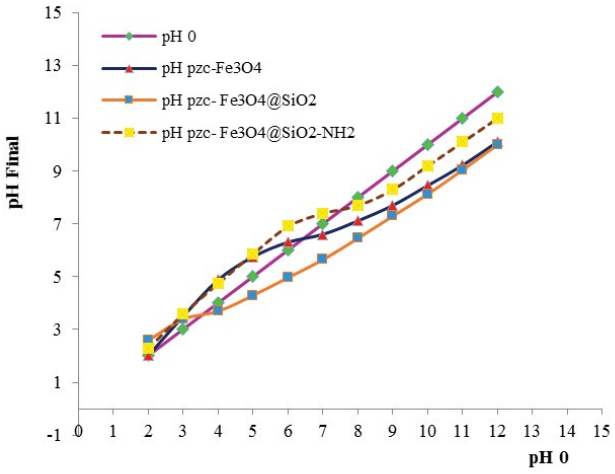

Fig. 4. Determination of pH pzc of Fe_3O_4, Fe_3O_4@SiO_2, and Fe_3O_4@SiO_2–APTES.

On the other hand, by increasing adsorbent dosage from 5 to 100 g L^{-1}, removal efficiency of Ni^{2+} was increased from 5% to 60% and from 20% to 80% for Fe_3O_4@SiO_2 and Fe_3O_4@SiO_2–APTES, respectively. In the same condition, Cd^{2+} removal efficiency 76% and 85% was observed for Fe_3O_4@SiO_2 and Fe_3O_4@SiO_2–APTES, respectively. Increasing removal efficiency with increasing adsorbent dosage can be related to increase of the number of available adsorption sites that lead to improving adsorption efficiency. Moreover, the high removal efficiency was observed at the 100 g L^{-1} adsorbent dosage and 50 ppm of initial Cd^{2+} and Ni^{2+} concentrations. The result shows that adsorption efficiency in Fe_3O_4@SiO_2–APTES is higher than Fe_3O_4@SiO_2 nanoparticles (70.5%, 90.5%). It is indicated that the modified surface of Fe_3O_4@SiO_2 by APTES lead to increasing electrostatic attraction and coordination could be ascribed to the high adsorption of metal ions [41]. Several studies have been carried out and the same result was achieved [41–45].

3.5. Isothermal studies of the adsorption

Langmuir and Freundlich equations were used for modeling these adsorption isotherm data which are presented in Table 1. Regression coefficients (R^2) of investigating

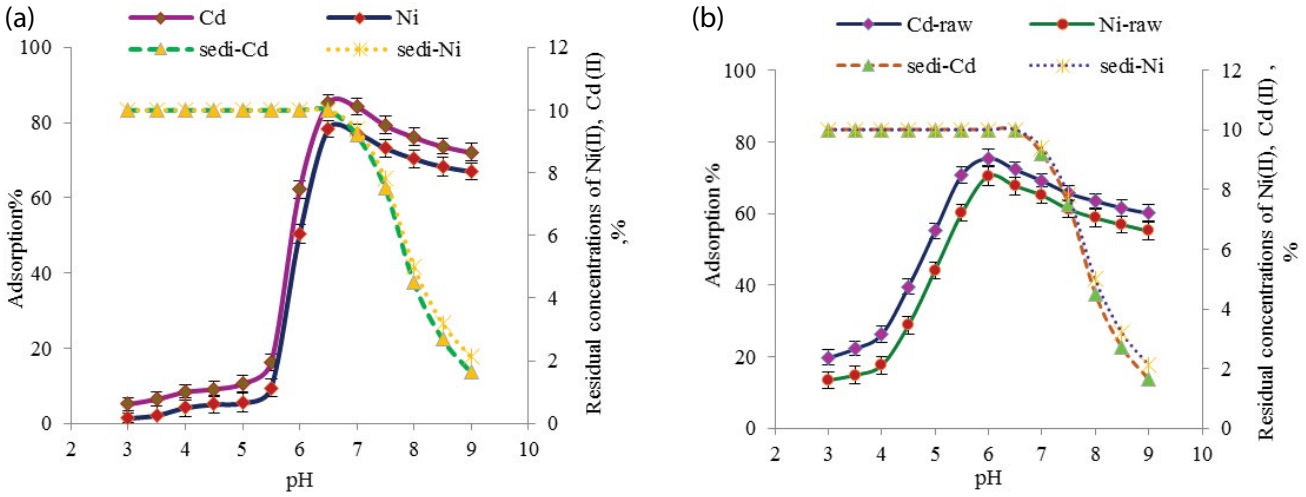

Fig. 5. Removal efficiency of Fe_3O_4@SiO_2 (a) and Fe_3O_4@SiO_2–APTES (b) on the adsorption of Cd^{2+} and Ni^{2+} in various initial pH.

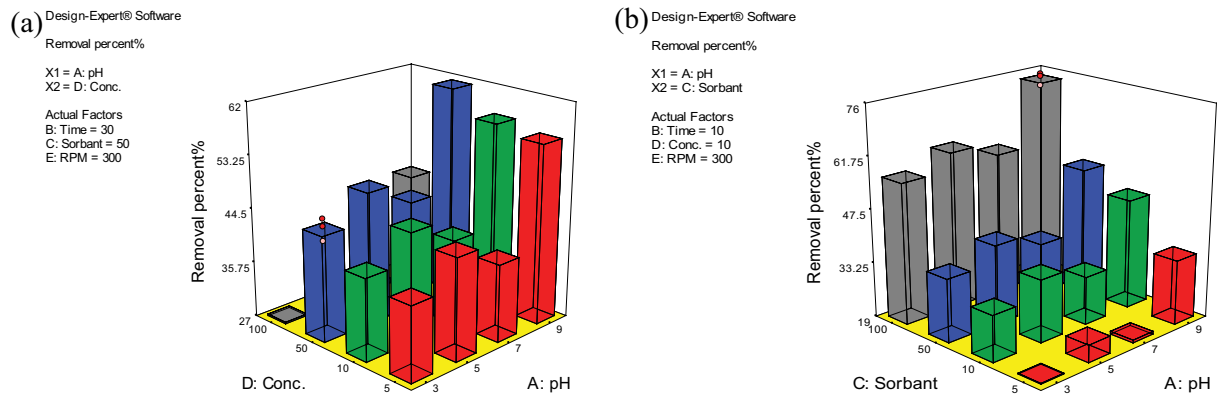

Fig. 6. Effect of pH and adsorbent dosage of Fe_3O_4@SiO_2 (a) and Fe_3O_4@SiO_2–APTES (b) on the removal efficiency of Cd^{2+} and, Ni^{2+}.

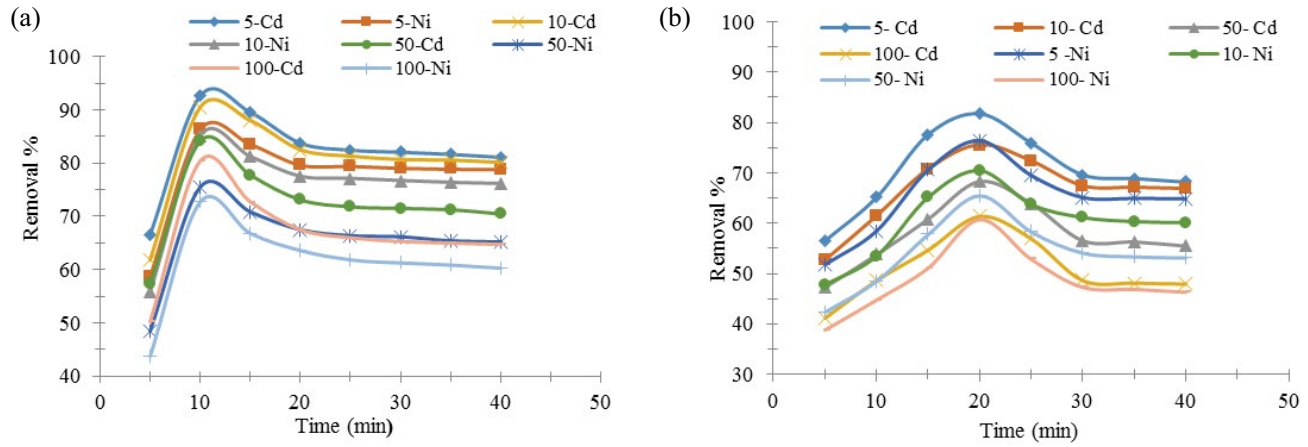

Fig. 7. Effect of contact time on Ni^{2+} and Cd^{2+} uptakes by $Fe_3O_4@SiO_2$ (a) and $Fe_3O_4@SiO_2$–APTES (b).

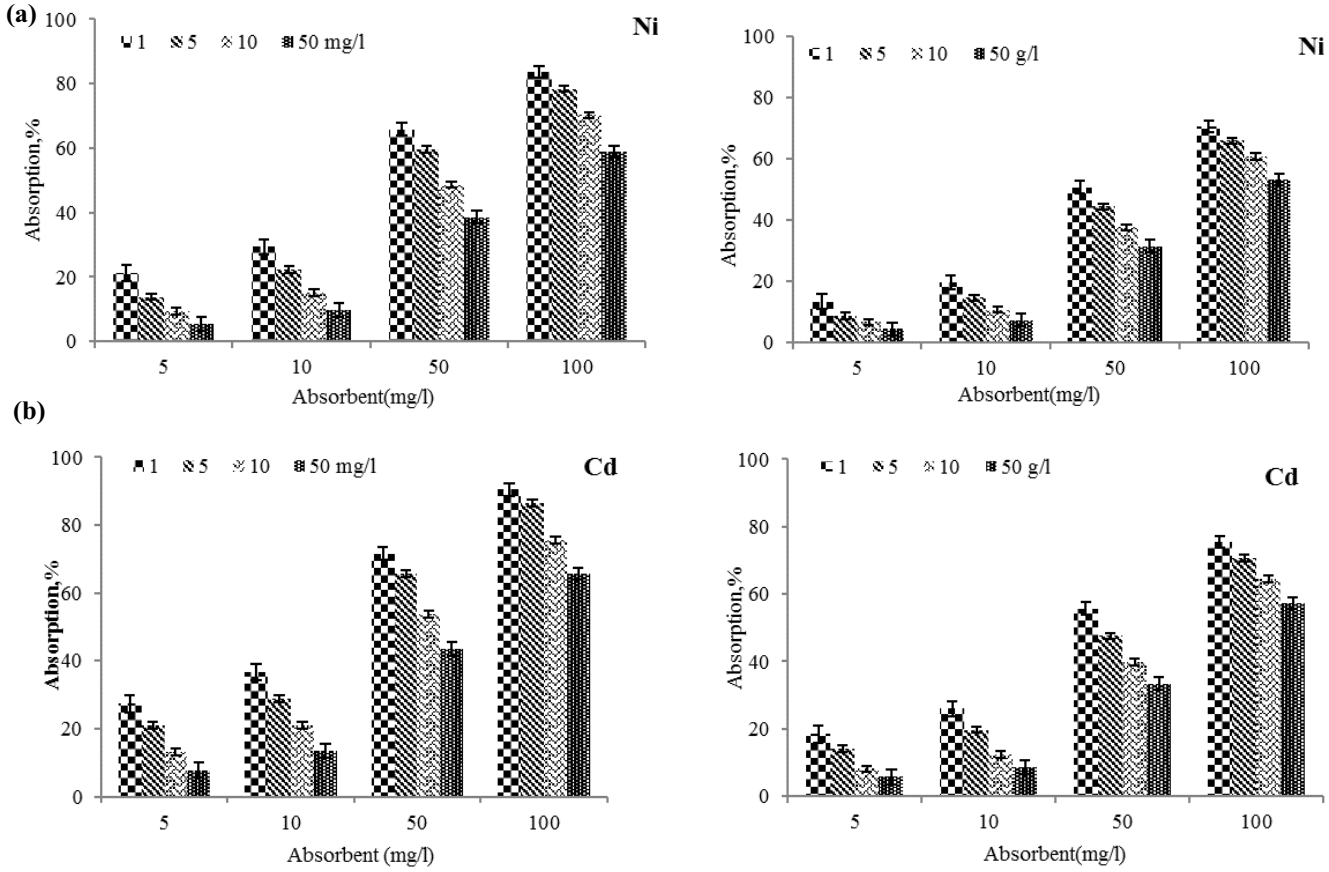

Fig. 8. Effect of adsorbent dose of $Fe_3O_4@SiO_2$ (a) and $Fe_3O_4@SiO_2$–APTES (b) on the adsorption of Ni(II), Cd(II).

adsorption isotherms were fitted with Langmuir isotherm with correlation coefficients (R^2) of 0.9973 (Figs. 9–12). So, the result has indicated that adsorption of Cd^{2+} on the $Fe_3O_4@SiO_2$ nanoparticle has structurally mono layer and the surface of the adsorbent surface is uniform. So, there is no interaction between adsorbed molecules [46,47]. According to Fig. 10, adsorption process of Ni^{2+} on the $Fe_3O_4@SiO_2$ nanoparticles can be well defined by both Langmuir and Freundlich isotherms with regression coefficients (R^2) of 0.97 and 0.98, respectively (Table 2). According to the data which are summarized in Table 2, maximum adsorption capacity q_m of Ni^{2+} and Cd^{2+} was obtained 18.88 and 17.3 mg/g, respectively. The value of sorption intensity (n) for the both of the sorbent is greater than unity ($n > 1$) so it is indicated that chemisorption process and mechanism of sorption is classified as L-type isotherms which is reflecting a high affinity

Table 1
Linear and non-linear isotherm equation

Isotherm	Non-linear equation	Linear equation
Langmuir-1		$\frac{C_e}{q_e}=\frac{C_e}{q_m}+\frac{1}{b\,q_e}$
Langmuir-2	$q_e=\frac{q_m b C_m}{1+b\,C_e}$	$\frac{1}{q_e}=\left(\frac{1}{bq_m}\right)\frac{1}{C_e}+\frac{1}{q_m}$
Langmuir-3		$q_e=q_m-\left(\frac{1}{b}\right)\frac{q_e}{C_e}$
Langmuir-4	$q_e=k_f C_e^{1/n}$	$\frac{q_e}{C_e}=bq_m-bq_m$
Freundlich	$q_e=K_F C_e^{1/n}$	$\ln\left(\frac{k_{pr}}{q_e}-1\right)-\beta\ln(C_e)+\ln(q_{RP})$

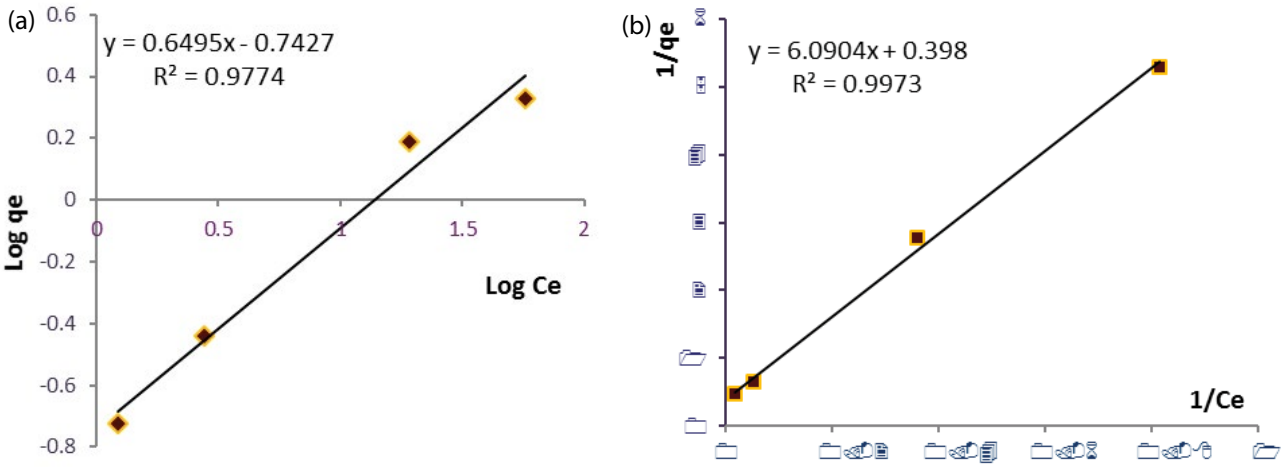

Fig. 9. Langmuir (a), Freundlich (b) adsorption isotherm of Cd^{2+} adsorption on Fe_3O_4@SiO_2.

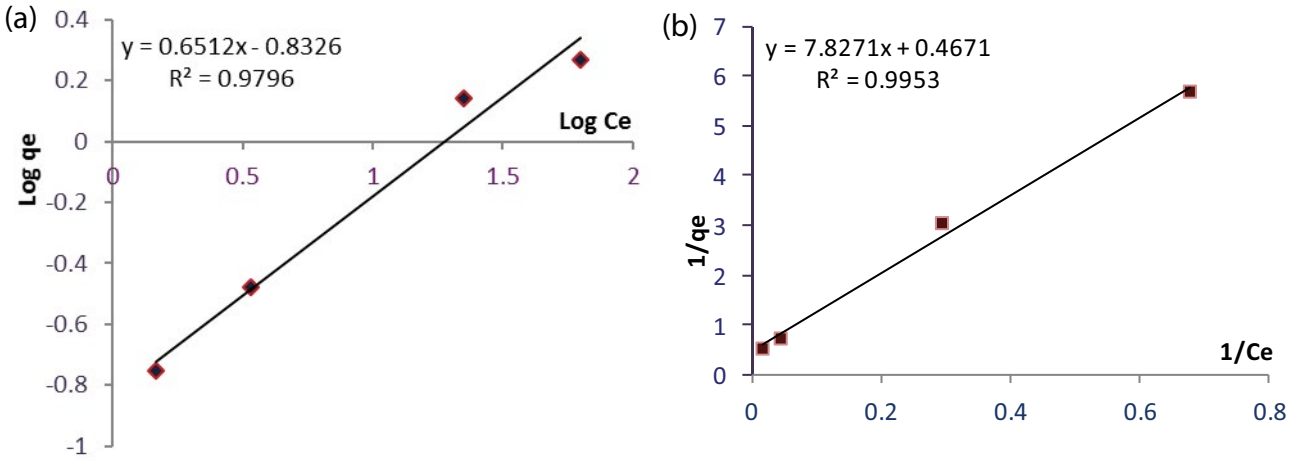

Fig. 10. Langmuir (a), Freundlich (b) adsorption isotherm of Ni^{2+} adsorption on Fe_3O_4@SiO_2.

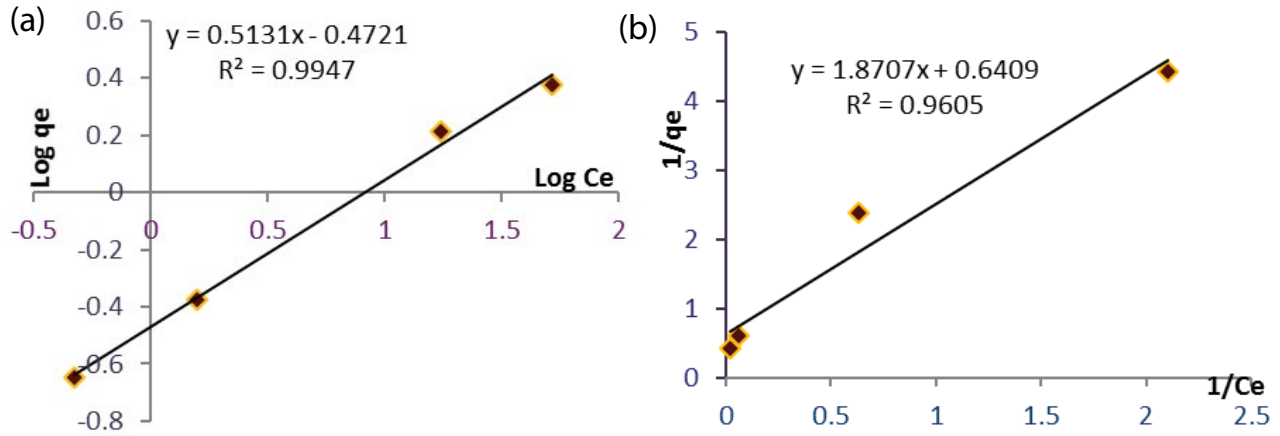

Fig. 11. Langmuir (a), Freundlich (b) adsorption isotherm of Cd^{2+} adsorption on Fe_3O_4@SiO_2–APTES.

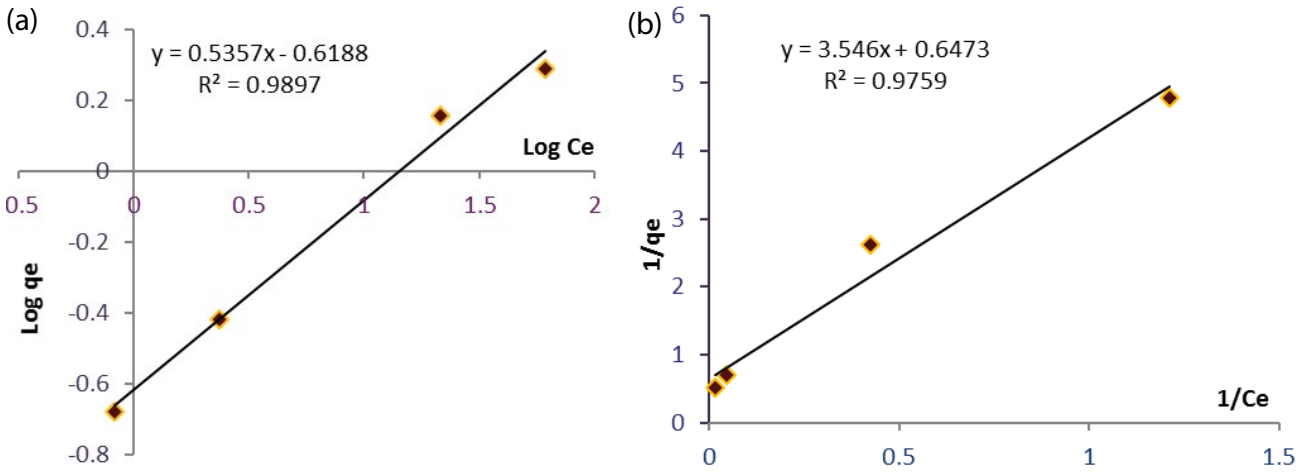

Fig. 12. Langmuir (a), Freundlich (b), adsorption isotherm of Ni^{2+} adsorption on Fe_3O_4@SiO_2–APTES.

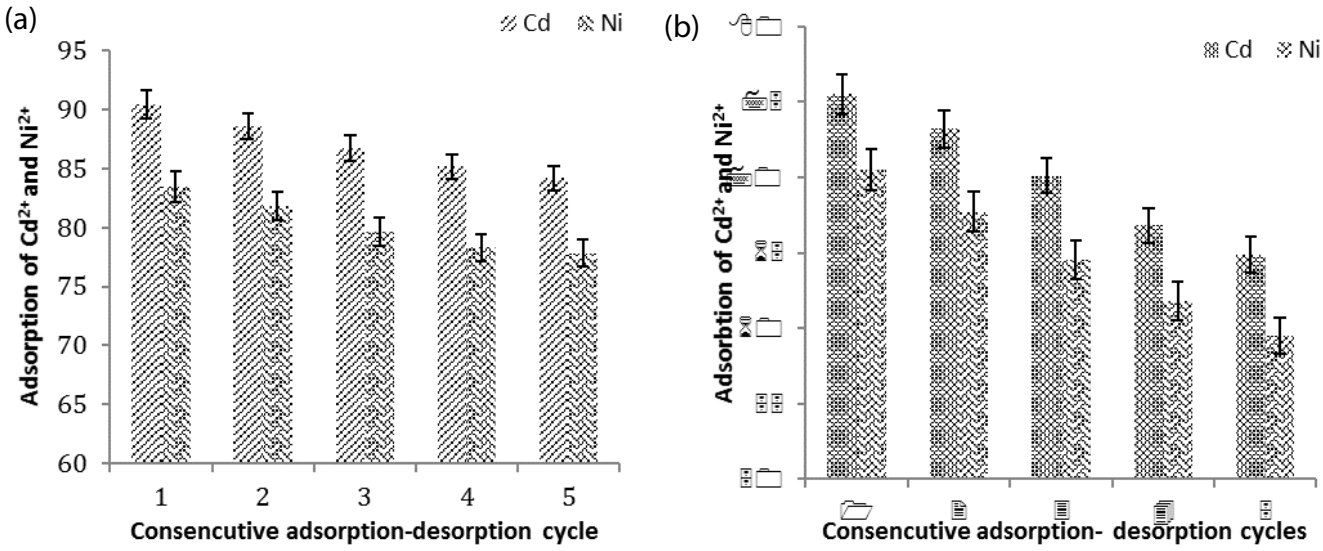

Fig. 13. Adsorption–desorption in consecutive cycles for Fe_3O_4@SiO_2 (a) and Fe_3O_4@SiO_2–APTES (b).

Table 2
Constants and correlation coefficients of adsorption isotherms for the Fe_3O_4@SiO_2 and Fe_3O_4@SiO_2–APTES

Adsorbent	Model	Parameter	Cd^{2+}	Ni^{2+}
Fe_3O_4@SiO_2	Freundlich equation	n	1.54	1.53
		q_m (mg/g)	–	–
		b (L/mg) = Kl	–	–
		K_f	0.18	1.14
		R^2	0.977	0.979
	Langmuir equation	n	–	–
		q_m (mg/g)	18.88	17.63
		b (L/mg) = Kl	0.068	0.06
		K_f		–
		R^2	0.9997	0.995
Fe_3O_4@SiO_2– APTES	Freundlich equation	n	1.94	1.86
		q_m (mg/g)	–	–
		b (L/mg) = Kl	–	–
		K_f	0.337	0.24
		R^2	0.995	0.976
	Langmuir equation	n	–	–
		q_m (mg/g)	18.88	17.63
		b (L/mg) = Kl	0.342	0.182
		K_f	–	–
		R^2	0.96	0.989

between adsorbate and adsorbent. In addition, based on the K_L and q_m values both of the adsorbents exhibited much higher affinity for Ni^{2+}ions than that of Cd^{2+}.

3.6. Desorption and reusability studies

Regeneration of the adsorbent for repeated use is of crucial importance in industrial practice for metal removal from wastewater [48–50]. Desorption experiments carried out with Cd^{2+} and Ni^{2+} for Fe_3O_4@SiO_2 and Fe_3O_4@SiO_2–APTES in 0.1 M HCl showed that approximately 90% and 94% of the adsorbed cadmium and nickel was desorbed. The results of the adsorption capacity of Fe_3O_4@SiO_2 and Fe_3O_4@SiO_2–APTES for five consecutive adsorption–desorption cycles are graphically illustrated in Figs. 13a and b.

4. Conclusion

The results presented show the efficiency of Fe_3O_4–SiO_2 and magnetic porous composites Fe_3O_4–SiO_2–APTES for the elimination of cadmium and nickel. According to the obtained data, the optimum conditions for the removal of 75.5% of cadmium and 70.5% of Ni^{2+} were obtained as follows: pH ≥ 5.5–6.5, initial concentration of Cd^{2+} and Ni^{2+}: 10 mg/L, time 20 min and 20 mg of Fe_3O_4–SiO_2, while in using of Fe_3O_4–SiO_2–APTES as an adsorbent 95.5% of cadmium and 83.5% of nickel were removed in the pH ≥ 6.5–7, 10 mg/L initial cadmium and nickel concentration, 20 mg adsorbent dosage and 10 min contact time. These facts encourage the use of Fe_3O_4–SiO_2–APTES as an environment friendly adsorbent in heavy metal removal. Certainly, further research is needed to allow for a more detailed economic evaluation.

Acknowledgments

The authors wish to extend special recognition to the Iran University of Medical Sciences for the financial support to carry out this project (No. 91-03-27-19494).

References

[1] M. Halim, P. Conte, A. Piccolo, Potential availability of heavy metals to phytoextraction from contaminated soils induced by exogenous humic substances, Chemosphere, 52 (2003) 265–275.
[2] M.I. Ansari, A. Malik, Biosorption of nickel and cadmium by metal resistant bacterial isolates from agricultural soil irrigated with industrial wastewater, Bioresour. Technol., 98 (2007) 3149–3153.
[3] L.R. Kalankesh, M.A. Zazouli, Removal of salt from the Caspian Sea using a single-and double-layer membrane microbial desalination cell in continuous-mode operation, Desal. Wat. Treat., 147 (2019) 83–89.
[4] L.R. Kalankesh, S. Rodríguez-Couto, Y.D. Shahamat, H.A. Asgarnia, Removal efficiency of nitrate, phosphate, fecal and total coliforms by horizontal subsurface flow-constructed wetland from domestic wastewater, Environ. Health Eng. Manage. J., 6 (2019) 105–111.
[5] L.R. Kalankesh, S. Rodríguez-Couto, M.A. Zazouli, Desalination and power generation of caspian sea by applying new designed microbial desalination cells in batch operation mode, Environ. Progr. Sustain. Energy, 38 (2019) 13205.
[6] R. Singh, N. Gautam, A. Mishra, R. Gupta, Heavy metals and living systems: an overview, Indian J. Pharmacol., 43 (2011) 246–253.
[7] X. Long, X. Yang, W. Ni, Current status and perspective on phytoremediation of heavy metal polluted soils, J. Appl. Ecol., 13 (2002) 757–762.
[8] A. Azimi, A. Azari, M. Rezakazemi, M. Ansarpour, Removal of heavy metals from industrial wastewaters: a review, ChemBioEng. Rev., 4 (2017) 37–59.

[9] Mahvi, F. Gholami, S. Nazmara, Cadmium biosorption from wastewater by Ulmus leaves and their ash, Euro. J. Sci. Res., 23 (2008) 203–197.
[10] E. Bazrafshan, L. Mohammadi, A. Ansari-Moghaddam, A.H. Mahvi, Heavy metals removal from aqueous environments by electrocoagulation process–a systematic review, J. Environ. Health Sci. Eng., 13 (2015) 74.
[11] A. Maleki, A.H. Mahvi, M.A. Zazouli, H. Izanloo, A.H. Barati, Aqueous cadmium removal by adsorption on barley hull and barley hull ash, Asian J. Chem., 23 (2011) 1373.
[12] L. Rafati, A. Mahvi, A. Asgari, S. Hosseini, Removal of chromium (VI) from aqueous solutions using Lewatit FO36 nano ion exchange resin, Int. J. Environ. Sci. Technol., 7 (2010) 147–156.
[13] M.R. Boldaji, A. Mahvi, S. Dobaradaran, S. Hosseini, Evaluating the effectiveness of a hybrid sorbent resin in removing fluoride from water, Int. J. Environ. Sci. Technol., 6 (2009) 629–632.
[14] M. Anjum, R. Miandad, M. Waqas, F. Gehany, M. Barakat, Remediation of wastewater using various nano-materials, Arabian J. Chem., 12 (2016) 4897–4919.
[15] Y.D. Shahamat, H. Asgharnia, L.R. Kalankesh, Data on wastewater treatment plant by using wetland method, Babol, Iran, Data Brief, 16 (2018) 1056–1061.
[16] F. Mansouri, R. Kalankesh, H. Hasankhani, The comparison of photo catalytic degradation of dissolved organic carbon (DOC) from water by UV/TiO_2 in the presence and absence of iron ion, Global Nest J., 18 (2016) 392–401.
[17] K. Zare, V.K. Gupta, O. Moradi, A.S.H. Makhlouf, M. Sillanpää, M.N. Nadagouda, H. Sadegh, R. Shahryari-Ghoshekandi, A. Pal, Z.-J. Wang, A comparative study on the basis of adsorption capacity between CNTs and activated carbon as adsorbents for removal of noxious synthetic dyes: a review. J. Nanostruct. Chem., 5 (2015) 227–236.
[18] S.H. Huang, M.H. Liao, D.H. Chen, Direct binding and characterization of lipase onto magnetic nanoparticles, Biotechnol. Prog., 19 (2003) 1095–1100.
[19] F. Mansouri, L.R. Kalankesh, H. Hasankhani, Removal of humic acid from contaminated water by nano-sized TiO–SiO, Adv. Biol. Res., 9 (2015) 58–65.
[20] M. Malakootian, L. Ranandeh Kalankesh, M. Loloi, Efficiency of hybrid nanoparticles of Tio_2/Sio_2 in removal of lead from paint industry effluents, JMUMS, 23 (2013) 244–254.
[21] M.H. Ehrampoush, M. Miria, M.H. Salmani, A.H. Mahvi, Cadmium removal from aqueous solution by green synthesis iron oxide nanoparticles with tangerine peel extract, J. Environ. Health Sci. Eng., 84 (2015) 13.
[22] M. Barakat, R. Kumar, Synthesis and characterization of porous magnetic silica composite for the removal of heavy metals from aqueous solution, J. Ind. Eng. Chem., 23 (2015) 93–99.
[23] M. Anbia, K. Kargosha, S. Khoshbooei, Heavy metal ions removal from aqueous media by modified magnetic mesoporous silica MCM-48, Chem. Eng. Res. Des., 93 (2015) 779–788.
[24] Q. Yuan, N. Li, Y. Chi, W. Geng, W. Yan, Y. Zhao, X. Li, B. Dong, Effect of large pore size of multifunctional mesoporous microsphere on removal of heavy metal ions, J. Hazard. Mater., 254 (2013) 157–165.
[25] Ren, X. Ding, W. Li, H. Wu, H. Yang, Highly efficient adsorption of heavy metals onto novel magnetic porous composites modified with amino groups, J. Chem. Eng. Data, 62 (2017) 1865–1875.
[26] J.K. Sahoo, A. Kumar, L. Rout, J. Rath, P. Dash, H. Sahoo, An investigation of heavy metal adsorption by hexa-dentate ligand-modified magnetic nanocomposites, Sep. Sci. Technol., 53 (2018) 863–876.
[27] A.P.H. Association, A.W.W. Association, Standard Methods for the Examination of Water and Wastewater, 1989: American Public Health Association.
[28] M. Ocaña, R. Rodriguez-Clemente, C.J. Serna, Uniform colloidal particles in solution: formation mechanisms, Adv. Mater., 7 (1995) 212–216.
[29] Z. Pourmanouchehri, M. Jafarzadeh, S. Kakaei, E.S. Khameneh, Magnetic nanocarrier containing 68 Ga–DTPA complex for targeted delivery of doxorubicin, J. Inorg. Organomet. Polym. Mater:, 28 (2018) 1980–1990.
[30] H. Qiu, B. Cui, G. Li, J. Yang, H. Peng, Y. Wang, N. Li, R. Gao, Z. Chang, Y. Wang, Novel Fe_3O_4@ ZnO@ $mSiO_2$ nanocarrier for targeted drug delivery and controllable release with microwave irradiation, J. Phys. Chem. C, 118 (2014) 14929–14937.
[31] X. Shen, Q. Wang, W. Chen, Y. Pang, One-step synthesis of water-dispersible cysteine functionalized magnetic Fe_3O_4 nanoparticles for mercury (II) removal from aqueous solutions, Appl. Surf. Sci., 317 (2014) 1028–1034.
[32] A. Idris, N.S.M. Ismail, N. Hassan, E. Misran, A.-F. Ngomsik, Synthesis of magnetic alginate beads based on maghemite nanoparticles for Pb (II) removal in aqueous solution, J. Ind. Eng. Chem., 18 (2012) 1582–1589.
[33] Uheida, M. Iglesias, C. Fontàs, Y. Zhang, M. Muhammed, Adsorption behavior of platinum group metals (Pd, Pt, Rh) on nonylthiourea-coated Fe_3O_4 nanoparticles, Sep. Sci. Technol., 41 (2006) 909–923.
[34] T. Cheng, M. Lee, M. Ko, T. Ueng, S. Yang, The heavy metal adsorption characteristics on metakaolin-based geopolymer, Appl. Clay Sci., 56 (2012) 90–96.
[35] S.S. Banerjee, D.-H. Chen, Fast removal of copper ions by gum arabic modified magnetic nano-adsorbent, J. Hazard. Mater., 147 (2007) 792–799.
[36] Wang, B. Wang, J. Liu, L. Yu, H. Sun, J. Wu, Adsorption of Cd (II) from acidic aqueous solutions by tourmaline as a novel material, Chin. Sci. Bull., 57 (2012) 3218–3225.
[37] Das, N. Mondal, R. Bhaumik, P. Roy, Insight into adsorption equilibrium, kinetics and thermodynamics of lead onto alluvial soil, Int. J. Environ. Sci. Technol., 11 (2014) 1101–1114.
[38] M. El-Awady, T. Sami, Removal of heavy metals by cement kiln dust, Bull. Environ. Contam. Toxicol., 59 (1997) 603–610.
[39] Namasivayam, K. Ranganathan, Removal of Cd (II) from wastewater by adsorption on "waste" Fe (III) Cr (III) hydroxide, Water Res., 29 (1995) 1737–1744.
[40] Y.-M. Hao, C. Man, Z.-B. Hu, Effective removal of Cu (II) ions from aqueous solution by amino-functionalized magnetic nanoparticles, J. Hazard. Mater., 184 (2010) 392–399.
[41] X. Xin, Q. Wei, J. Yang, L. Yan, R. Feng, G. Chen, B. Du, H. Li, Highly efficient removal of heavy metal ions by amine-functionalized mesoporous Fe_3O_4 nanoparticles, J. Chem. Eng., 184 (2012) 132–140.
[42] Erdem, G. Çölgeçen, R. Donat, The removal of textile dyes by diatomite earth, Colloid Interface Sci., 282 (2005) 314–319.
[43] X. Wang, K. Maeda, A. Thomas, K. Takanabe, G. Xin, J.M. Carlsson, K. Domen, M. Antonietti, A metal-free polymeric photocatalyst for hydrogen production from water under visible light, Nat. Mater., 8 (2009) 76.
[44] K. Jayaram, I. Murthy, H. Lalhruaitluanga, M. Prasad, Biosorption of lead from aqueous solution by seed powder of *Strychnos potatorum* L. Colloids Surf., B, 71 (2009) 248–254.
[45] K. Jayaram, M. Prasad, Removal of Pb (II) from aqueous solution by seed powder of *Prosopis juliflora* DC, J. Hazard. Mater., 169 (2009) 991–997.
[46] R. Schmid, C.N. Reilley, A rapid electrochemical method for the determination of metal chelate stability constants, ACS, 78 (1956) 5513–5518.
[47] R. Kumar, J. Chawla, Removal of cadmium ion from water/wastewater by nano-metal oxides: a review, Water Qual. Expo. Health, 5 (2014) 215–226.
[48] H.J. Mansoorian, A.H. Mahvi, A.J. Jafari, Removal of lead and zinc from battery industry wastewater using electrocoagulation process: influence of direct and alternating current by using iron and stainless steel rod electrodes, Sep. Purif. Technol., 135 (2014) 165–175.
[49] Kakavandi, R.R. Kalantary, M. Farzadkia, A.H. Mahvi, A. Esrafili, A. Azari, A.R. Yari, A.B. Javid, Enhanced chromium (VI) removal using activated carbon modified by zero valent iron and silver bimetallic nanoparticles, J. Environ. Health Sci. Eng., 12 (2014) 115.
[50] Bazrafshan, A.H. Mahvi, M.A. Zazouli, Removal of zinc and copper from aqueous solutions by electrocoagulation technology using iron electrodes, Asian J. Chem., 23 (2011) 5506.